Malaysian Journal Of Civil Engineering

Full Paper

SPECTRAL FATIGUE ANALYSIS PROCEDURE FOR JACKET OFFSHORE STRUCTURES

Samsul Imran Bahrom[a,d,*], Mohd Khairi Abu Husain[a], Mohamad Shazwan Ahmad Shah[b], Ezanizam Mat Soom[c], Noor Irza Mohd Zaki[a]

[a]Faculty of Artificial Intelligence, Universiti Teknologi Malaysia, Jalan Sultan Yahya Petra, 54100 Kuala Lumpur, Malaysia
[b]Faculty of Civil Engineering, Universiti Teknologi Malaysia, 81310 UTM Johor Bahru, Johor, Malaysia
[c]PTTEP JDX & PC JDA Joint Operations Sdn. Bhd., Jalan Pinang, 50450 Kuala Lumpur, Malaysia
[d]McDermott Asia Pacific Sdn. Bhd., Subsea & Floating Facilities, Menara Hap Seng 2, Jalan P. Ramlee, 50250 Kuala Lumpur, Malaysia

Article history
Received
01 October 2025
Received in revised form
20 December 2025
Accepted
22 December 2025
Published online
31 March 2026

*Corresponding author
samsulimran@graduate.utm.my

Abstract

Fatigue remains a critical design and assessment challenge for offshore jacket structures operating under cyclic wave loading throughout their service life. Spectral fatigue analysis offers a robust framework for assessing cumulative damage by combining environmental loading spectra with the dynamic response of structures. This article presents and demonstrates a structured spectral fatigue analysis procedure for jacket platforms, implemented using SACS software in accordance with ISO 19902 and API RP 2A guidelines. The procedure encompasses model calibration with hydrodynamic coefficients and corrosion allowances, derivation of the Centre of Damage (CoD) wave, equivalent linearization of soil–pile interaction, evaluation of natural frequency and mode shape, wave response simulations, transfer function generation and fatigue life estimation using the Palmgren–Miner rule. Application to a 54.5 m water depth jacket platform highlights critical hot-spot stresses at tubular joints, with one joint exhibiting a fatigue life of only 12.94 years. The novelty of this study lies in bridging theoretical formulations with explicit software-based implementation, offering a transparent, stepwise framework that links metocean data, structural dynamics and fatigue assessment outputs. The proposed methodology contributes to advancing best practices for offshore structural design and integrity management, providing a replicable reference for both academic research and industrial applications.

Keywords: Spectral fatigue analysis; Offshore jacket structures; Fatigue life prediction; Wave response analysis; Soil–pile interaction

1.0 INTRODUCTION

Offshore jacket platforms are some of the most commonly used fixed structures in the oil and gas industry, as well as in emerging renewable energy sectors. These structures operate in harsh marine environments where waves, wind and currents continually load critical structural members (Ahmad Saharuddin et al., 2024). Over time, this loading causes fatigue damage, which is a leading cause of decline and possible failure in offshore steel structures (Abu Husain et al., 2014; Syed Ahmad et al., 2022). Therefore, fatigue assessment is crucial for maintaining long-term structural integrity, reducing failure risks and extending the safe operational life of these assets (Erfani, 2022; Vuong & Quan, 2019).

Traditional fatigue evaluations have often depended on deterministic methods that use representative sea states or simplified load histories. Although these methods provide valuable insights, they do not fully reflect the random nature of environmental loading (Martínez et al., 2025; Mukhlas et al., 2023). In contrast, spectral fatigue analysis offers a more robust framework (Kvittem, 2014). It combines wave energy spectra with stressl transfer functions and natural frequencies to

quantify cumulative fatigue damage (Damilola et al., 2021; Nallayarasu et al., 2010). This method enables a stochastic assessment that takes into account both the variability of sea states and the structure's dynamic response.

Several factors influence the accuracy of spectral fatigue predictions. These include hydrodynamic load modelling, soil–pile interaction, stress concentration factors (SCFs) and wave scatter distributions (Muis Alie, 2016; Mat Soom et al., 2018). Specifically, the fatigue performance of tubular joints is sensitive to SCFs, which increase nominal stresses at welded connections (American Petroleum Institute, 2014). Additionally, the nonlinear behaviour of soil–pile interaction requires equivalent linearization for accurate dynamic response evaluation within modal superposition frameworks (Azman et al., 2021).

Commercial software such as SACS has become a standard tool for fatigue evaluation in the offshore industry. It integrates hydrodynamics, structural dynamics and fatigue life assessment within one integrated software solution (Zwerneman & Digre, 2010). However, while ISO 19902 (International Organization for Standardization, 2020) and API RP 2A-WSD (American Petroleum Institute, 2014) offer general guidelines for fatigue design and reassessment, they do not provide detailed step-by-step implementation workflows. This often results in inconsistencies, particularly in projects within regions of limited offshore engineering experience (Kraedegh et al., 2024).

To fill this gap, this study develops a detailed spectral fatigue analysis procedure for jacket offshore structures, implemented within SACS software and in line with international standards. The procedure covers hydrodynamic model adjustments, determination of the Centre of Damage (CoD) wave, equivalent linearization of soil–pile interaction, evaluation of natural period and mode shape, generation of static and dynamic transfer functions, wave response analysis and fatigue life prediction using the Palmgren–Miner rule, which is a widely used method for cumulative damage assessment (Kelma & Schaumann, 2015; Nicola et al, 2024).

This work connects theoretical formulations with clear software implementation steps, offering a transparent and replicable guide for spectral fatigue evaluation. In this way, the study serves as a valuable reference for researchers and practitioners seeking to enhance offshore structural design and integrity management.

2.0 REVIEW OF FATIGUE ANALYSIS IN OFFSHORE JACKET STRUCTURES

Fatigue has long been recognised as one of the most critical issues for offshore jacket structures. Since these platforms are subjected to continuous cyclic wave loading throughout their operational life, fatigue cracks at welded tubular joints are often the primary source of structural deterioration (Shabakhty & Tabatabaei, 2021). In severe cases, they can even lead to premature failure. Earlier approaches to fatigue assessment were mainly deterministic. Engineers used a few representative sea states or simplified load histories to estimate fatigue life. While these methods were practical and less computationally demanding, they tended to oversimplify the randomness of ocean waves, which could lead to misleading results (Sarpkaya & Isaacson, 1981; Ahmad Saharuddin et al., 2024).

The industry gradually shifted towards spectral fatigue analysis, which treats the problem in a probabilistic sense by combining wave energy spectra with the structure's transfer functions and natural periods. This method enables the estimation of fatigue damage from the full range of sea states, rather than from a limited set of conditions (Wirsching, 1984; Moan, 2018). Because it accounts for variability in both the environment and the structural response, spectral fatigue analysis has become the preferred approach for jackets in harsh marine environments, as well as for reassessing ageing assets.

Several design standards have helped guide this transition. ISO 19902 (International Organization for Standardization, 2020) outlines the requirements for fatigue design and reassessment of fixed steel offshore structures, while API RP 2A-WSD (American Petroleum Institute, 2014) provides recommended practices for hydrodynamic modelling, SCF estimation and fatigue design curves. More recently, DNVGL-RP-C203 (DNV, 2017) has provided a detailed framework for fatigue design of offshore steel structures, with attention to uncertainties in material properties, S–N curves and metocean data. Even so, these standards stop short of prescribing exact computational steps, leaving engineers to interpret and implement the procedures with tools such as SACS or SESAM.

On the academic side, several studies have examined spectral fatigue in more detail. Nallayarasu et al. (2010) applied the method to jacket structures in the Mumbai High field, showing how wave scatter data and directional sea states strongly influence fatigue damage predictions. Their work underlined that fatigue life is highly sensitive to tubular joint geometry and wave directionality. Similarly, Moan (2018) reflected on lessons from the Alexander Kielland accident, stressing the importance of reliability-based fatigue assessment over the full life cycle of marine structures.

One of the key technical challenges in fatigue analysis is the role of stress concentration factors (SCFs). Because fatigue cracks almost always start at welded joints, the accuracy of SCF predictions is central to the analysis. The widely used formulae developed by Efthymiou (1988) remain the basis for estimating hotspot stresses in tubular joints and these equations are still referenced in most industry guidelines.

Another critical factor is the interaction between the soil and the pile. Since jacket structures rely on piles for stability, the way the soil reacts under cyclic wave loading directly affects the platform's dynamic response (Shabakhty & Tabatabaei, 2021; Ayob et al., 2014). Soil behaviour is nonlinear, which complicates its use in dynamic analysis. To overcome this, engineers often rely on equivalent linearisation methods to generate stiffness matrices, a process supported by the PSI module in SACS (Jung et al, 2020; DNV, 2017).

The availability of commercial software such as SACS has made spectral fatigue analysis more accessible in routine engineering practice. These tools combine hydrodynamic loading, modal analysis, stress transfer function generation and fatigue damage evaluation in a single workflow. However, the software manuals tend to focus on "which button to press" rather than clearly explaining the theoretical basis (Wan Alwi et al., 2019). As a result, many users treat the process as a black box, without fully understanding the connections between the theory, the standards, and the program's inputs and outputs (Feng & Large, 2010).

On the one hand, there are highly theoretical works that explain the mathematics of spectral fatigue, but they provide

little guidance on implementation. There are software-specific manuals that show how to run the analysis, but they provide little explanation of the underlying principles. There are few studies that attempt to bridge these two worlds by presenting a transparent, step-by-step methodology that connects international standards, theoretical background and practical software execution in a single place (Jung et al., 2020).

This study attempts to fill that gap. By developing a structured spectral fatigue analysis procedure for jacket offshore structures and implementing it in SACS. The aim is to make the process more transparent and replicable. This procedure brings together all the essential components of the analysis, from hydrodynamic model adjustments and soil–pile linearisation to transfer functions, wave response and fatigue life estimation.

3.0 TEST STRUCTURE SPECIFICATION AND ENVIRONMENTAL CONDITION

The case study considered in this paper is a jacket-type offshore platform installed in a water depth of approximately 54.5 meters. The structure is supported by conductor piles that are grouted within the annulus of the jacket legs, providing the foundation stability required to resist long-term environmental loading. While the platform model reflects typical features of fixed offshore jackets, it is used here primarily as a demonstration example to illustrate the step-by-step procedure of spectral fatigue analysis. The purpose is not to conduct a detailed design verification of the structure, but rather to demonstrate how the methodology can be applied in practice. A three-dimensional view of the jacket is shown in Figure 1.

The spectral fatigue analysis depends on metocean data that characterize the long-term environmental conditions at the platform site, including waves, wind and currents (Yak et al., 2022). For wave loading, conditions are represented through a wave scatter diagram, which shows the distribution of significant wave heights (H_s) and peak periods (T_p) across a range of short-term sea states (refer to Figure 2). In addition, the directional distribution of wave occurrences is presented in Figure 3, since the angle of wave approach plays an essential role in the fatigue response of jacket structures.

The metocean data used in this study are provided for demonstration purposes only. The values are illustrative and are not intended to represent actual field measurements or to be used for design verification. Instead, they serve to support the explanation of the spectral fatigue analysis procedure outlined in this study.

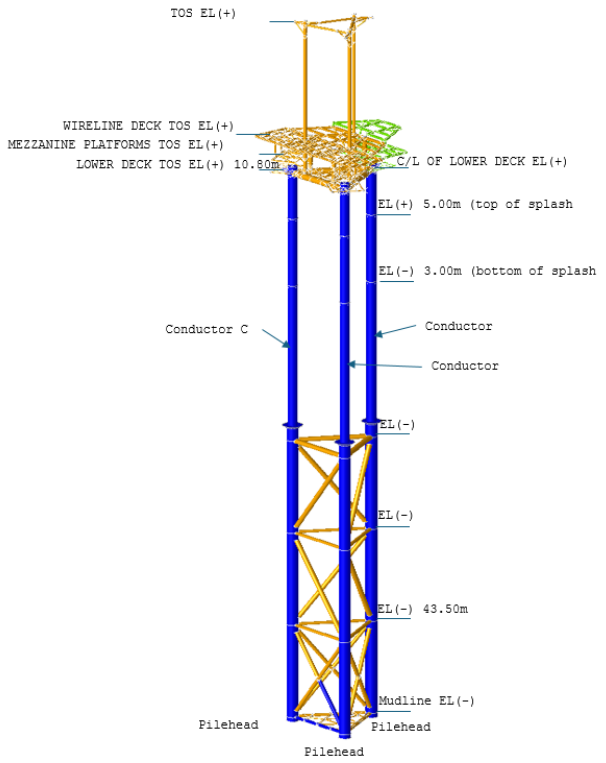

Figure 1 3D view of jacket structure.

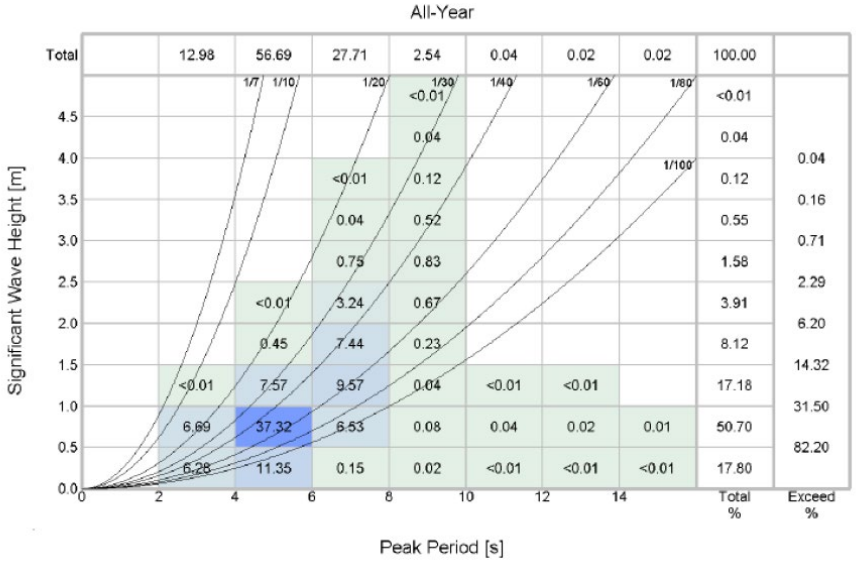

Figure 2 Percentage occurrence of significant wave height against peak period – all year.

Figure 3 Percentage occurrence of significant wave height against direction – all year.

4.0 METHODOLOGY

The spectral fatigue analysis conducted in this study broadly follows the framework described in ISO 19902 (International Organization for Standardization, 2020), with several simplifications and adjustments made to make the process more practical for implementation in SACS. The overall procedure is illustrated in Figure 4 and the main steps are described here.

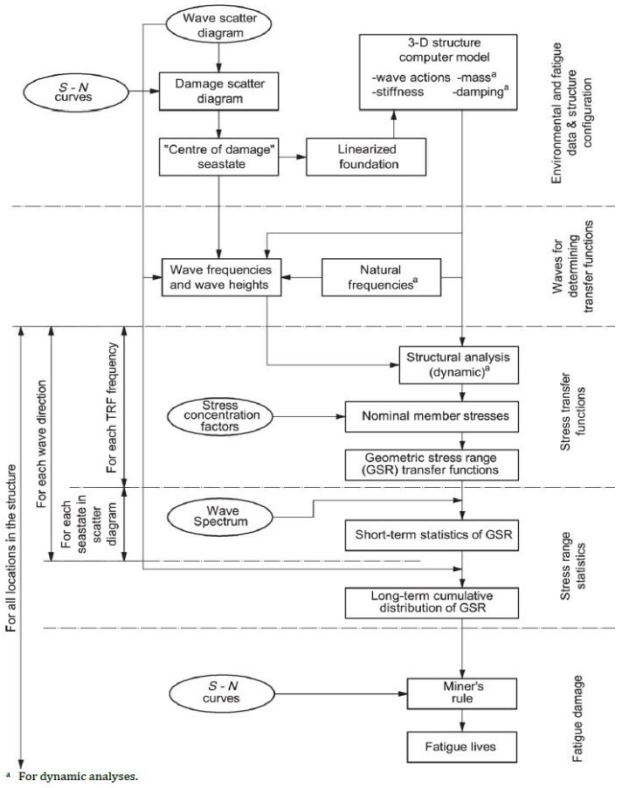

Figure 4 Flowchart of spectral fatigue analysis procedure.

The first requirement is the preparation of environmental and fatigue input data. Wave scatter diagrams are used to capture the long-term metocean conditions at the site, showing how significant wave height and peak period vary across different sea states and directions. This information, together with the chosen S–N curve, forms the basis for the fatigue calculations. In this case, the WJT curve from API RP 2A-WSD was selected, as it is widely applied for welded tubular joints in jackets.

From the scatter diagram, a representative Centre of Damage (CoD) sea state is calculated. This is the wave condition that contributes most to fatigue damage, obtained by weighting wave heights and periods according to their expected influence on fatigue (Zaki et al., 2014; Zhang & Sun, 2020). The CoD wave is beneficial for simplifying the modelling of soil–pile behaviour, which is inherently nonlinear. In SACS, this nonlinear behavior is handled through the PSI module, which produces an equivalent linear stiffness matrix, allowing the pile-soil system to be incorporated into the jacket model.

With the linearized foundation established, the structure's dynamic properties are determined using the DYNPAC module. The natural frequencies and mode shapes are extracted by solving an eigenvalue problem for the complete jacket. This step is critical because fatigue is strongly influenced by whether the wave loading spectrum overlaps with the structure's natural periods. For this case study, the first two natural modes were found to be 3.88 and 3.87 seconds, respectively, which lie within the range of typical wave periods at the site.

The next step involves generating base shear transfer functions using the SEASTATE module for all wave directions over a frequency range of 0.1 to 1.0 Hz. The peaks and valleys of each transfer function are identified and recorded as "important frequencies."

These frequencies, together with additional points near the structure's natural periods and their multiples, are then used in the DYNAMIC RESPONSE module to perform a full response analysis. This ensures that resonance effects, where the response can be amplified, are appropriately captured. The resulting analysis produces detailed stress and displacement

data for each wave direction, which are stored in Common Solution Files (CSFs)..

The last step uses the FATIGUE module, which reads the Common Solution Files (CSFs) to calculate cumulative fatigue damage. In this step, the stress response spectrum is generated by multiplying the square of the dynamic stress transfer functions by the selected wave spectrum (Pierson–Moskowitz). The resulting spectrum represents the distribution of stress variance across frequencies. The Stress Concentration Factors (SCFs), derived from Efthymiou's parametric equations, are then applied to obtain the true hotspot stresses. These stresses are assessed against the appropriate WJT S–N curve, with thickness correction applied as specified in the design code (American Petroleum Institute, 2014), to compute fatigue life. Finally, the Palmgren–Miner rule is used to determine cumulative damage, where a damage ratio of 1.0 corresponds to the end of the joint's fatigue life.

The outcome of this process is an estimate of the fatigue life for each joint in the structure. The results are presented in both listing files and interactive fatigue plots in SACS, which allow critical locations to be identified quickly. In this study, the most vital location was found at brace 1117–1015, with a predicted fatigue life of 12.94 years at the chord face, indicating that this joint is the most vulnerable point in the structure.

4.1 Modification of In-Place Structural Model

The first step in the analysis is to adjust the hydrodynamic coefficients of the structural model so that it is suitable for fatigue assessment, using values different from those in the in-place analysis. According to the guidelines in API RP 2A-WSD (American Petroleum Institute, 2014), various values are adopted for the drag coefficient (C_d) depending on the surface condition of the members: C_d = 0.8 is applied for rough members and C_d = 0.5 for smooth members. The inertia coefficient (C_m) is taken as 2.0 for all members.

In addition to these adjustments, a corrosion allowance is introduced to account for long-term material degradation. This is typically applied by reducing the wall thickness of tubular members, often by half of the value used in the in-place strength analysis. Incorporating corrosion allowance ensures that the hydrodynamic loading and structural capacity used in the fatigue model reflect more realistic conditions expected over the service life of the platform.

4.2 Centre of Damage (CoD) Calculation

The Centre of Damage (CoD) wave is used to represent the sea state that contributes most significantly to fatigue damage. Instead of analysing all possible combinations of wave height and period individually, the CoD provides a single representative condition that reflects the weighted influence of the full wave scatter data (refer to Table 1).

To calculate the CoD, the significant wave height (H_s) and peak period (T_p) are obtained as weighted averages across all sea states. The weighting is based on the relative damage contribution (D_i) of each sea state, which depends on both the probability of occurrence and its expected fatigue effect. Mathematically, this can be expressed as (Mat Soom et al., 2024):

$$H_s = \frac{\sum D_i H_i}{\sum D_i} \quad (1)$$

$$T_p = \frac{\sum D_i T_i}{\sum D_i} \quad (2)$$

where, D_i is the contribution (or damage factor) of each sea state, H_i is the significant wave height and T_i is the peak period.

Once the representative H_s and T_p are obtained, the corresponding maximum wave height (H_{max}) and associated period with the maximum wave height period (T_{max}) are derived using standard wave relations.

$$H_{max} = 1.8H_s \quad (3)$$

$$T_{max} = 1.005T_p \quad (4)$$

These values are then used in subsequent analyses, particularly in the soil–pile interaction modelling and transfer function generation.

Table 1 Wave scatter diagram datasheet.

Di (x1000) (Pi*Hi^3/Ti)		Ti(s)																	TOTAL
		1.00	3.00	5.00	7.00	9.00	11.00	13.00	15.00	17.00	19.00	21.00	23.00	25.00	27.00	29.00	31.00	33.00	
Hi (m)	8.75																		0.000
	8.25																		0.000
	7.75																		0.000
	7.25																		0.000
	6.75																		0.000
	6.25																		0.000
	5.75																		0.000
	5.25																		0.000
	4.75					0.3572													0.357
	4.25					3.2412													3.241
	3.75				0.2260	6.7382													6.964
	3.25				1.7164	19.6431													21.360
	2.75				22.2821	19.1791													41.461
	2.25			0.0683	52.7218	8.4163													61.206
	1.75			4.8234	56.9619	1.3696													63.155
	1.25		0.0065	29.5700	26.7017	0.0868	0.0018	0.0015											56.368
	0.75		9.4077	31.4884	3.9355	0.0375	0.0153	0.0078	0.0039										44.896
	0.25		0.3271	0.3547	0.0033	0.0003	0.0000	0.0000	0.0000										0.685
Total		0.0000	9.7413	66.3049	164.5488	59.0695	0.0171	0.0093	0.0039										299.695

4.3 Equivalent Linearization of Nonlinear Soil-Pile Interaction

The interaction between piles and surrounding soil is inherently nonlinear, as soil stiffness depends on load level, displacement, and cyclic degradation. However, SACS performs dynamic analysis using linear modal superposition, which means that fully nonlinear soil models cannot be directly incorporated. To overcome this limitation, the foundation is simplified using an equivalent linear representation, a well-established practice in offshore engineering that balances accuracy with computational efficiency (DNV, 2017).

This equivalent model is generated through the Pile–Soil Interaction (PSI module) in SACS. The module creates a stiffness matrix (super-element) that reflects the overall response of the pile–soil system under representative loading. In this study, the representative condition was defined using the Centre of Damage (CoD) wave, characterised by the maximum wave height (H_{max}) and associated period (T_{max}) identified in Section 4.2. By applying these loads, the soil response could be linearised in a way that preserves its influence on structural dynamics while remaining compatible with the spectral fatigue framework.

Both lateral and axial stiffness components were obtained from the pile displacements calculated under the CoD loading. Two approaches are commonly used in practice: stiffness values can be based on the AVG method, where pilehead loads and displacements from the selected PSI load cases are used and the resulting pilehead stiffnesses are averaged across all similar piles and all selected load cases, or on the MAX method, which uses the maximum pilehead displacement of any pile in the selected load case. In either case, the aim is to ensure that the equivalent springs adequately capture the soil restraint without overestimating or underestimating the foundation flexibility.

Figure 5 shows an excerpt from the PSI input file used in this study, demonstrating how the equivalent stiffness properties were defined and embedded into the jacket structural model. By adopting this approach, the analysis realistically represents soil–pile effects within the constraints of a linear dynamic system, providing a practical compromise between theoretical accuracy and computational feasibility.

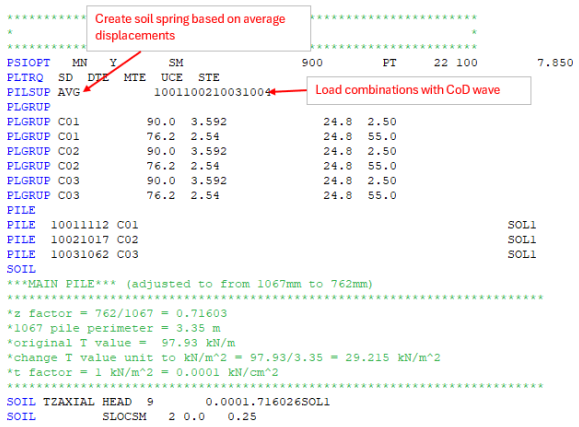

Figure 5 Excerpt from PSI input file.

4.4 Dynamic Analysis (Natural Period and Mode Shapes)

Understanding the natural frequencies and mode shapes of a jacket platform is crucial in fatigue analysis, as these properties determine how the structure will respond when subjected to cyclic wave loading. If the frequency of incoming waves is close to one of the structure's natural frequencies, resonance may occur, leading to amplified stresses and accelerated fatigue damage.

In this study, the jacket model was analysed with the equivalent linear soil springs described earlier (Section 4.3) so that the effects of the foundation were realistically included in the dynamic behaviour. The dynamic analysis was performed using the DYNPAC module in SACS, which solves the system as an eigenvalue problem, where the stiffness matrix, mass matrix, and displacement vector define the natural frequencies and the manner in which the structure deforms at each frequency. The resulting eigenvalues provide the natural frequencies, while the corresponding eigenvectors describe the mode shapes.

The following equation of motion governs the dynamic behaviour of the structure for undamped free vibration:

$$[K]\{X\} - \omega^2[M]\{X\} = 0 \quad (5)$$

where, K is the stiffness matrix, which includes the effects of both the structure and the soil springs derived from the CoD wave, M is the mass matrix, ω represents the circular natural frequency (rad/s), and X is the mode shape vector.

Solving this equation provides the Eigenvalues, which correspond to the natural frequencies of the structure. The associated Eigenvectors describe the mode shapes, which illustrate how the structure deforms at each natural frequency. The natural period (T_n) of the structure is calculated as the inverse of the natural frequency (f_n):

$$T_n = \frac{1}{f_n} \quad (6)$$

The natural periods and mode shapes are critical inputs to the wave response analysis (Section 4.6), which evaluates the structure's response to wave loading. Specifically, these natural frequencies help identify potential resonance conditions where the structure's response could be amplified, leading to greater cyclic stresses and fatigue. The natural periods of the structure obtained from the analysis (refer to Figure 6) indicate that the first and second modes are nearly identical, with values of 3.88 and 3.87 seconds, respectively, and typically represent the fundamental sway modes in the global X and Y directions, while the third and fourth modes are significantly shorter, at 1.34 and 1.32 seconds, respectively, and are commonly associated with torsional or higher-order response.

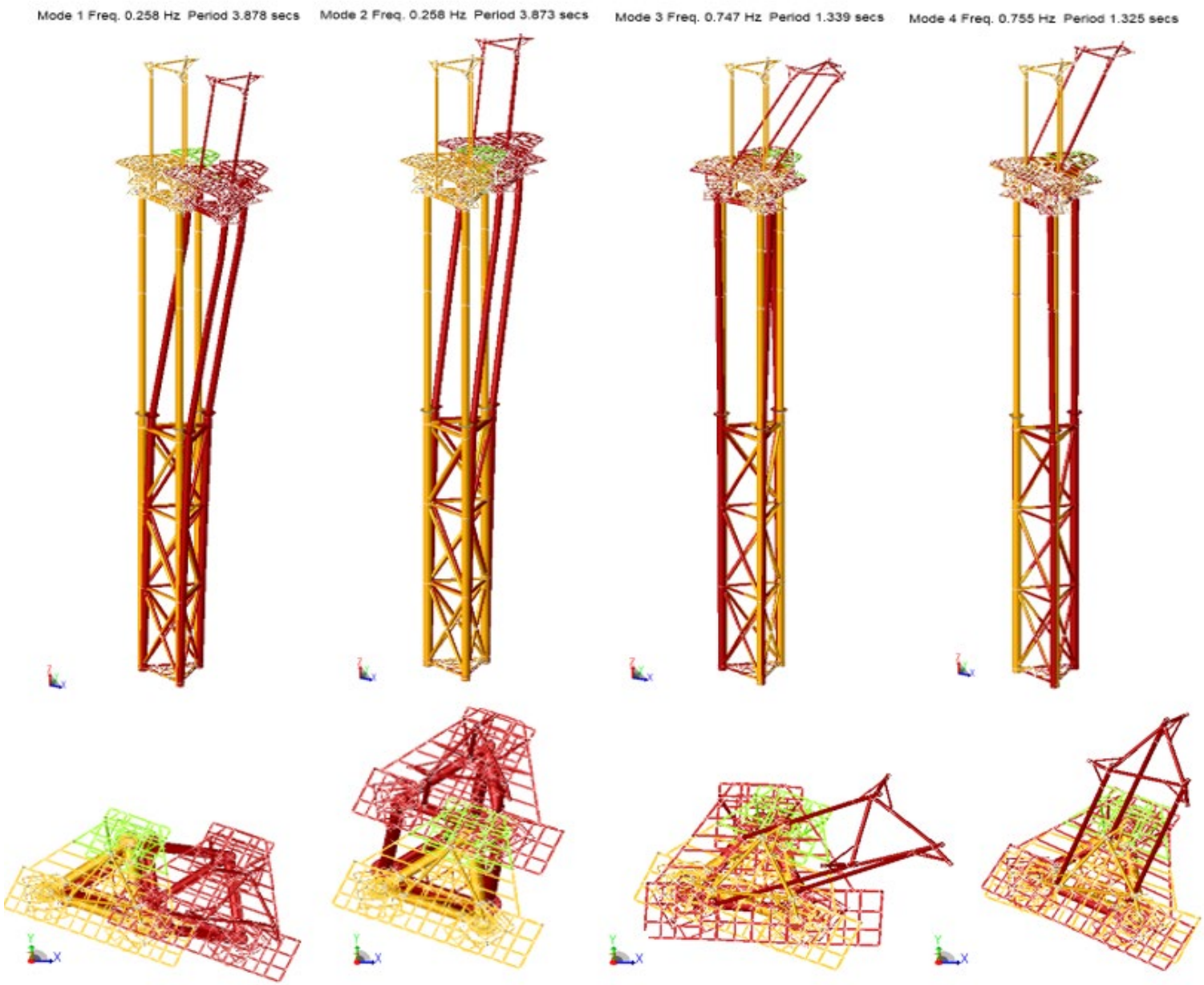

Figure 6 First four mode shapes of the jacket structure, illustrating the dominant global deformation patterns governing the dynamic response used in the spectral fatigue analysis.

4.5 Wave Loading Analysis and Base Shear Transfer Function Generation

The next step in the procedure is to determine the variation of global base shear across different frequencies and directions. This was carried out using the SEASTATE module in SACS, with analyses performed for a range of wave approach angles (i.e., 0°, 45°, 90°, 135°, 225°, 270°, and 316°). The output from this analyses is a set of base shear transfer functions, which describe the relationship between wave frequency and resulting base shear for each direction. These transfer functions effectively illustrate how base shear varies with frequency which serves as a key input to the subsequent wave response analysis.

For this study, base shear transfer functions were generated over a frequency range of 0.1 Hz to 1.0 Hz, which corresponds to wave periods between 1 and 10 seconds. To ensure realistic wave loading, the wave heights used in the transfer function generation were derived from the wave steepness, defined as:

$$H = LS \tag{7}$$

where, H is the wave height, L is the wavelength calculated from the relation $L = 1.56T^2$ (with T as the wave period) and S is wave steepness.

In practice, wave steepness typically falls within the range of 1:15 to 1:25 depending on site conditions. For the CoD wave identified earlier, the steepness was calculated as approximately 1:21, based on H_{max} = 3.47 m and T_{max} = 6.86 s. This value was adopted in the present analysis. The SEASTATE input file for the generation of the static transfer function in the present study is shown in Figure 7.

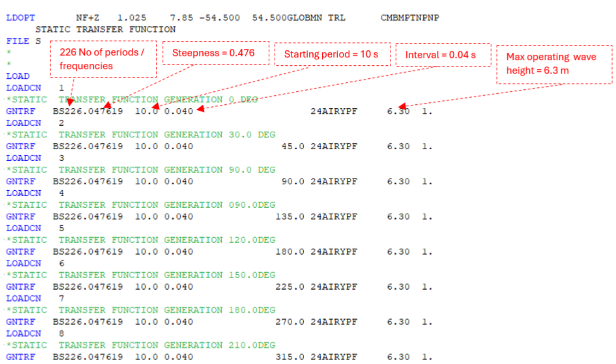

```
LDOPT        NF+Z    1.025     7.85 -54.500   54.500GLOBMN TRL       CMBMPTNPNP
     STATIC TRANSFER FUNCTION
FILE S
*
*
LOAD
LOADCN   1
*STATIC  TRANSFER FUNCTION GENERATION 0 DEG
GNTRF    BS226.047619  10.0 0.040                        24AIRYPF     6.30  1.
LOADCN   2
*STATIC  TRANSFER FUNCTION GENERATION 30.0 DEG
GNTRF    BS226.047619  10.0 0.040                   45.0 24AIRYPF     6.30  1.
LOADCN   3
*STATIC  TRANSFER FUNCTION GENERATION 90.0 DEG
GNTRF    BS226.047619  10.0 0.040                   90.0 24AIRYPF     6.30  1.
LOADCN   4
*STATIC  TRANSFER FUNCTION GENERATION 090.0DEG
GNTRF    BS226.047619  10.0 0.040                  135.0 24AIRYPF     6.30  1.
LOADCN   5
*STATIC  TRANSFER FUNCTION GENERATION 120.0DEG
GNTRF    BS226.047619  10.0 0.040                  180.0 24AIRYPF     6.30  1.
LOADCN   6
*STATIC  TRANSFER FUNCTION GENERATION 150.0DEG
GNTRF    BS226.047619  10.0 0.040                  225.0 24AIRYPF     6.30  1.
LOADCN   7
*STATIC  TRANSFER FUNCTION GENERATION 180.0DEG
GNTRF    BS226.047619  10.0 0.040                  270.0 24AIRYPF     6.30  1.
LOADCN   8
*STATIC  TRANSFER FUNCTION GENERATION 210.0DEG
GNTRF    BS226.047619  10.0 0.040                  315.0 24AIRYPF     6.30  1.
END
```


Figure 7 Input file for the generation of static transfer functions.

An example of the output is shown in Figure 8, which illustrates the base shear transfer function for the 0° wave direction. A critical consideration in this step is the selection of frequencies for the dynamic wave response analysis. If the frequency grid is too coarse, the peaks and valleys of the transfer functions may be missed, leading to inaccurate stress predictions. For this reason, additional frequency points were included around the natural periods of the structure to capture resonance effects more accurately.

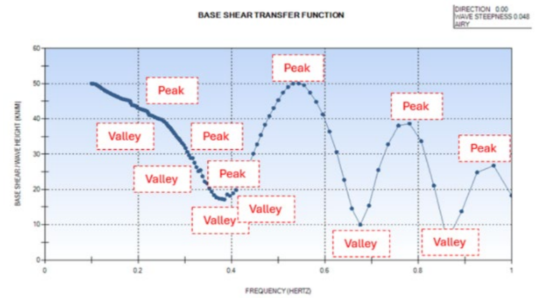

Figure 8 Transfer Function for 0-degree wave direction.

Following the recommendations of API RP 2A-WSD (American Petroleum Institute, 2014), additional frequency points were selected close to the structure's natural period (f_n) and its multiples. This step is essential because resonance effects can significantly amplify structural response, and using only standard frequency intervals may overlook these critical peaks. In this study, frequencies at $0.95f_n$, $0.98f_n$, $1.02f_n$, and $1.05f_n$ were included to capture the behaviour around the first natural mode more accurately. The final set of periods ($T = 1/f$ chosen for the wave response analysis is summarised in Table 2.

Table 2 Chosen periods for wave response analysis

Sea State	Period T	L =1.56 T^2	Steepnes	H L x steepne	H_{used}	S_{used}	Remarks
1	10.00	156.00	0.048	7.43	6.300	0.040	Ending Period
2	9.96	154.75	0.048	7.37	6.300	0.041	
3	9.88	152.28	0.048	7.25	6.300	0.041	
4	9.80	149.82	0.048	7.13	6.300	0.042	
5	9.76	148.60	0.048	7.08	6.300	0.042	
6	9.72	147.39	0.048	7.02	6.300	0.043	
7	9.68	146.18	0.048	6.96	6.300	0.043	
8	9.60	143.77	0.048	6.85	6.300	0.044	
9	8.55	114.04	0.048	5.43	5.430	0.048	
10	7.50	87.75	0.048	4.18	4.179	0.048	
.	.	.	.	.	.	.	
.	.	.	.	.	.	.	
17	4.03	25.34	0.048	1.21	1.206	0.048	1.04*T1
18	3.96	24.46	0.048	1.16	1.165	0.048	1.02*T1
19	3.95	24.34	0.048	1.16	1.159	0.048	1.02*T2
20	3.92	23.97	0.048	1.14	1.142	0.048	
21	3.88	23.48	0.048	1.12	1.118	0.048	T1= Period 1st Mode
22	3.87	23.36	0.048	1.11	1.113	0.048	T2= Period 2nd Mode
23	3.80	22.53	0.048	1.07	1.073	0.048	0.98 *T1
24	3.76	22.05	0.048	1.05	1.050	0.048	
25	3.72	21.59	0.048	1.03	1.028	0.048	0.96 * T1
26	3.68	21.13	0.048	1.01	1.006	0.048	
27	3.64	20.67	0.048	0.98	0.984	0.048	
56	1.40	3.06	0.048	0.15	0.305	0.100	
57	1.39	3.01	0.048	0.14	0.305	0.101	1.04*T3
58	1.38	2.97	0.048	0.14	0.305	0.103	1.04*T4
59	1.37	2.93	0.048	0.14	0.305	0.104	1.02*T3
60	1.35	2.84	0.048	0.14	0.305	0.107	1.02*T4
61	1.34	2.80	0.048	0.13	0.305	0.109	T3= Period 3rd Mode
62	1.32	2.72	0.048	0.13	0.305	0.112	T4= Period 4th Mode
63	1.31	2.68	0.048	0.13	0.305	0.114	0.98*T3
64	1.30	2.64	0.048	0.13	0.305	0.116	0.98*T4
65	1.29	2.60	0.048	0.12	0.305	0.117	0.96*T3
66	1.27	2.52	0.048	0.12	0.305	0.121	0.96*T4
.	.	.	.	.	.	.	
.	.	.	.	.	.	.	
72	1.00	1.56	0.048	0.07	0.305	0.196	Beginning Period

Periods chosen for wave response

4.6 Wave Response Analysis

The purpose of the wave response analysis, performed using the DYNAMIC RESPONSE module, is to determine the stress ranges in the jacket structure that arise from the wave frequencies identified in the transfer function study (Section 4.5). These stress ranges form the basis for fatigue damage calculations. To capture the actual dynamic behaviour of the platform, the mode shapes and natural frequencies obtained earlier (Section 4.4) are incorporated into the analysis.

The structural response to wave loading can be expressed through the general equation of motion:

$$[K]\{X\} + [C]\{X'\} - \omega^2[M]\{X''\} = \{F\} \qquad (8)$$

where, X' is the velocity, X'' is the acceleration and F is the applied external force

An example input file for 0 degrees used for wave response analysis is shown in Figure 9. Input files for other wave directions follow a similar format but are not shown here. In this study, a 2% damping was considered. Using this formulation, SACS computes the stress responses for each selected sea state and wave direction, producing dynamic transfer function plots that show how the platform reacts to cyclic loading across the frequency spectrum.

```
LDOPT   IN  NF+Z   1.025   7.850 -54.500  54.500GLOBMN DYN       CMBMPT
*               DYNAMIC TRANSFER FUNCTION
FILE S
*
LOADCN  1
GNTRF   AL  1  0.040 10.00 10.00                   24AIRYPF    6.300 1.0
GNTRF   AL  1  0.041  9.96  9.96                   24AIRYPF    6.300 1.0
GNTRF   AL  1  0.041  9.88  9.88                   24AIRYPF    6.300 1.0
GNTRF   AL  1  0.042  9.80  9.80                   24AIRYPF    6.300 1.0
GNTRF   AL  1  0.042  9.76  9.76                   24AIRYPF    6.300 1.0
GNTRF   AL  1  0.043  9.72  9.72                   24AIRYPF    6.300 1.0
GNTRF   AL  1  0.043  9.68  9.68                   24AIRYPF    6.300 1.0
GNTRF   AL  1  0.044  9.60  9.60                   24AIRYPF    6.300 1.0
GNTRF   AL  1  0.048  8.55  8.55                   24AIRYPF          1.0
GNTRF   AL  1  0.048  7.50  7.50                   24AIRYPF          1.0
GNTRF   AL  1  0.048  6.45  6.45                   24AIRYPF          1.0
GNTRF   AL  1  0.048  5.40  5.40                   24AIRYPF          1.0
GNTRF   AL  1  0.048  5.36  5.36                   24AIRYPF          1.0
GNTRF   AL  1  0.048  4.92  4.92                   24AIRYPF          1.0
GNTRF   AL  1  0.048  4.47  4.47                   24AIRYPF          1.0
GNTRF   AL  1  0.048  4.25  4.25                   24AIRYPF          1.0
GNTRF   AL  1  0.048  4.03  4.03                   24AIRYPF          1.0
GNTRF   AL  1  0.048  3.96  3.96                   24AIRYPF          1.0
GNTRF   AL  1  0.048  3.95  3.95                   24AIRYPF          1.0
GNTRF   AL  1  0.048  3.92  3.92                   24AIRYPF          1.0

GNTRF   AL  1  0.109  1.34  1.34                   24AIRYPF          1.0 0.305
GNTRF   AL  1  0.112  1.32  1.32                   24AIRYPF          1.0 0.305
GNTRF   AL  1  0.114  1.31  1.31                   24AIRYPF          1.0 0.305
GNTRF   AL  1  0.116  1.30  1.30                   24AIRYPF          1.0 0.305
GNTRF   AL  1  0.117  1.29  1.29                   24AIRYPF          1.0 0.305
GNTRF   AL  1  0.121  1.27  1.27                   24AIRYPF          1.0 0.305
GNTRF   AL  1  0.127  1.24  1.24                   24AIRYPF          1.0 0.305
GNTRF   AL  1  0.145  1.16  1.16                   24AIRYPF          1.0 0.305
GNTRF   AL  1  0.156  1.12  1.12                   24AIRYPF          1.0 0.305
GNTRF   AL  1  0.168  1.08  1.08                   24AIRYPF          1.0 0.305
GNTRF   AL  1  0.181  1.04  1.04                   24AIRYPF          1.0 0.305
GNTRF   AL  1  0.196  1.00  1.00                   24AIRYPF          1.0 0.305
END
```

Determined from Section 4.5

Figure 9 Sea state Input File for wave response analysis 0 degrees.

Once the wave response analysis is complete, the results can be examined through dynamic transfer function plots. An example of the 0° wave direction is shown in Figure 10. The plot illustrates the variation of base shear with wave frequency, expressed in kN/m against Hz. As expected, the response curve shows a clear peak at approximately 0.257 Hz, which corresponds closely to the structure's first natural period of 3.88 seconds. This alignment confirms that the model successfully captures the resonance behaviour of the jacket under wave loading. Transfer function plots for other wave directions were also generated, but are not presented here for brevity.

The outputs from this stage are stored in Common Solution Files (CSFs), which contain beam member end forces and stresses. These files are critical for the subsequent fatigue analysis, where the stress ranges are combined with scatter diagram data and S–N curves to estimate fatigue life.

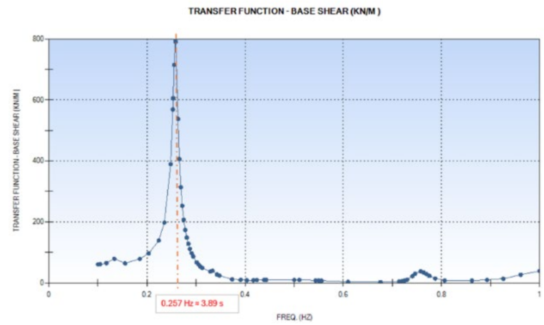

Figure 10 Dynamic Transfer Function plot 0 degrees.

4.7 Fatigue Analysis

The fatigue evaluation in SACS is carried out using the FATIGUE module with a dedicated fatigue input file (FTGINP), which specifies the parameters governing the analysis. The following elements were defined for this study:

i. Wave Scatter Data:
Long-term metocean conditions were represented using a wave scatter diagram, which defines the percentage occurrence of sea states based on significant wave height and peak period for different directions. These percentages are converted into a fraction of the design life within the fatigue input file, so that each sea state contributes proportionally to the cumulative damage calculation. This approach simplifies the random nature of the sea environment into a manageable set of conditions while retaining the statistical variability that drives fatigue damage (DNV, 2017).

ii. S–N Curve:
The Welded Joint Tubular (WJT) curve was selected to represent the fatigue resistance of the platform's critical connections. The WJT curve is widely recommended for jacket structures, as fatigue failure in these platforms most often initiates at welded tubular joints. While alternative S–N curves exist (e.g., for plain plate or ground welds), the WJT curve provides the most conservative and representative basis for tubular joint assessment (American Petroleum Institute, 2014; International Organization for Standardization, 2020).

iii. Stress Concentration Factors (SCFs):
Local stress amplification effects were accounted for using the Efthymiou parametric equations, a method that estimates SCFs based on joint geometry and loading. This approach remains widely used in offshore design practice and is recommended by ISO 19902 (International Organization for Standardization, 2020) and API RP 2A-WSD (American Petroleum Institute, 2014). Incorporating SCFs ensures that fatigue life predictions reflect hot-spot stresses at tubular joints, rather than relying solely on nominal member stresses (Efthymiou, 1988).

iv. Wave Spectrum:
The Pierson–Moskowitz (PM) spectrum was adopted to describe the distribution of wave energy across frequencies. The PM spectrum is suitable for fully developed seas, where wind has acted over a long fetch and duration, and is frequently used in offshore fatigue assessments. Although other spectra, such as JONSWAP, may better represent fetch-limited seas, PM provides a

conservative and widely accepted option (Mohd Zaki et al., 2014).

By defining these inputs, the FTGINP file ensures that the spectral fatigue analysis captures both the long-term variability of the marine environment and the structural response characteristics most critical to fatigue performance. This setup provides a robust framework for estimating the cumulative fatigue damage of offshore jacket structures.

4.7.1 Fatigue Input File

An excerpt from the fatigue input file (FTGINP) used in this study is presented in Figure 11. The figure highlights the key parameters defined for the fatigue analysis, including the selected S–N curve, the stress concentration factors (SCFs), the wave spectrum, as well as the wave heights and directional distributions. These inputs collectively ensure that the fatigue calculations reflect both the environmental conditions and the structural details critical to fatigue performance.

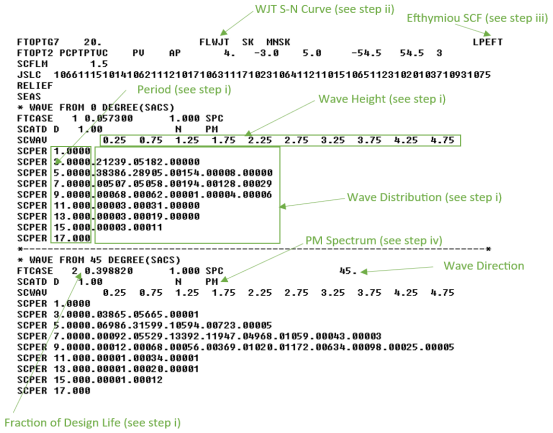

Figure 11 Excerpt from fatigue input file.

To demonstrate how the input data are applied in practice, Table 3 (a to c) presents the detailed calculation of the frequency of occurrence for FTCASE1 (SACS wave angle = 0°). This case was selected as an illustrative example because wave loading along the principal axis of the jacket often governs the fatigue response, particularly for critical joints aligned with the wave direction. By showing FTCASE1 in detail, the process of translating long-term metocean data from the scatter diagram (Section 4.2) into specific load cases for spectral fatigue analysis is clearly demonstrated.

Table 3 Wave distribution calculation for 0 degrees (FTCASE 1).

a) Normalized data presented in Figure 2.

		Ti(s)																	TOTAL
		1.00	3.00	5.00	7.00	9.00	11.00	13.00	15.00	17.00	19.00	21.00	23.00	25.00	27.00	29.00	31.00	33.00	
Hi (m)	8.75																		
	8.25																		
	7.75																		
	7.25																		
	6.75																		
	6.25																		
	5.75																		
	5.25																		
	4.75					1.0000													1.0000
	4.25					1.0000													1.0000
	3.75				0.0254	0.9746													1.0000
	3.25				0.0636	0.9364													1.0000
	2.75				0.4747	0.5253													1.0000
	2.25			0.0008	0.8291	0.1702													1.0000
	1.75			0.0554	0.9163	0.0283													1.0000
	1.25		0.0001	0.4406	0.5569	0.0023	0.0001	0.0001											1.0000
	0.75		0.1320	0.7361	0.1288	0.0016	0.0008	0.0005	0.0003										1.0000
	0.25		0.3527	0.6375	0.0084	0.0011	0.0001	0.0001	0.0001										1.0000

0.3527 = 6.28 / 17.80
(Refer Figure 2)

b) Normalized data presented in Figure 3.

SACS ANGLE	135 °	90 °	45 °	0 °	315 °	270 °	225 °	180 °	TOTAL
Hs (m)	DIRECTIONAL PERCENTAGE OF WAVES FROM THE FOLLOWING SECTORS								
	N	NE	E	SE	S	SW	W	NW	
0.25	0.2559	0.0682	0.1096	0.6021	0.3125	0.1385	0.1337	0.2516	1.872
0.75	0.5224	0.2906	0.4293	0.3927	0.6296	0.7236	0.6327	0.5252	4.146
1.25	0.1599	0.2401	0.2405	0.0035	0.0543	0.1323	0.1852	0.1422	1.158
1.75	0.0533	0.1963	0.1304	0.0014	0.0035	0.0055	0.0373	0.0547	0.482
2.25	0.0021	0.1188	0.0599	0.0003	0.0001	0.0001	0.0090	0.0109	0.201
2.75	0.0021	0.0556	0.0223				0.0013	0.0109	0.092
3.25	0.0021	0.0227	0.0068				0.0003	0.0011	0.033
3.75	0.0021	0.0059	0.0010				0.0003	0.0011	0.010
4.25		0.0017	0.0003				0.0003	0.0011	0.003
4.75		0.0002	0.0001					0.0011	0.001
5.25									0.000
5.75									0.000
6.25									0.000
6.75									0.000
7.25									0.000
7.75									0.000
8.25									0.000
8.75									0.000
TOTAL	1.0000	1.0000	1.0000	1.0000	1.0000	1.0000	1.0000	1.0000	

0.6021 = 3.45 / 5.72
(Refer Figure 3)

c) Wave distribution for FTCASE 1 (SACS angle = 0 degrees, True Direction SE).

Tp		SE Direction SACS Angle = 0.00 Hs (m)																		TOTAL
		0.25	0.75	1.25	1.75	2.25	2.75	3.25	3.75	4.25	4.75	5.25	5.75	6.25	6.75	7.25	7.75	8.25	8.75	
1.00																				0.0000
3.00		0.2124	0.0518																	0.2642
5.00		0.3839	0.2891	0.0015	0.0001															0.6745
7.00		0.0051	0.0506	0.0019	0.0013	0.0003														0.0592
9.00		0.0007	0.0006		0.0000	0.0001														0.0014
11.00		0.0000	0.0003																	0.0003
13.00		0.0000	0.0002																	0.0002
15.00		0.0000	0.0001																	0.0001
17.00																				0.0000
19.00																				0.0000
21.00																				0.0000
23.00																				0.0000
25.00																				0.0000
27.00																				0.0000
29.00																				0.0000
31.00																				0.0000
33.00																				0.0000
		0.60209	0.39267	0.00349	0.00140	0.00035														1.0000

0.2124 =0.3527 x 0.6021

4.7.2 Fatigue Damage Calculation

The final stage of the spectral fatigue analysis is the calculation of cumulative fatigue damage at critical joints of the jacket. This is carried out using the Palmgren–Miner linear damage rule, which assumes that fatigue failure occurs when the sum of damage fractions from all contributing stress cycles reaches unity. In this framework, each stress cycle consumes a portion of the joint's fatigue life and the total damage is obtained by summing contributions across all sea states and stress ranges. The stress range and fatigue damage are computed based on the following formulations:

$$\sigma_{RMS_i} = \sqrt{\int_0^\infty H^2(f) S_i(f) df} \tag{9}$$

where, σ_{RMS_i} is the root mean square stress for the *i-th* seastate, $H(f)$ is the transfer function between stress and wave elevation and $S_i(f)$ is the spectral density of the *i-th* seastate, corresponding to the wave direction being considered.

and

$$D = \frac{N}{\sigma_{RMS_i}^2} \int_0^\infty \frac{s}{N_F(s)} exp\left\{-\frac{s^2}{2\sigma_{RMS_i}^2}\right\} ds \tag{10}$$

where, D is the accumulated damage for the *i-th* seastate and wave direction, N is the number of stress cycles experienced during the sea state, $N_F(s)$ is the number of cycles to failure based on the S-N curve and s is the stress range. The total expected fatigue damage over the design life of the structure is obtained by summing the damage contributions from all sea states, weighted by their respective probabilities of occurrence.

4.7.3 Fatigue Damage Calculation

To capture the localised effects of fatigue at tubular joints, the stresses obtained in Section 4.7.2 are evaluated at eight designated hot-spot locations on each connection, as illustrated in Figure 12. These hot-spot locations are prescribed in offshore design practice, as they represent the regions most susceptible to fatigue cracking.

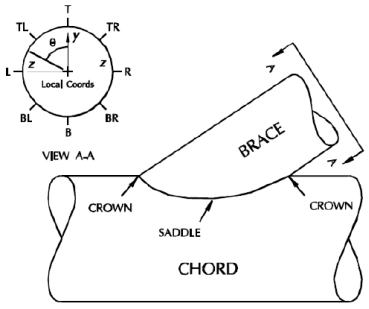

Figure 12 Stress points on tubular connections.

At each stress point, a Stress Concentration Factor (SCF) is applied to account for the geometric and loading-induced amplification of stresses in the vicinity of the weld. The SCFs are calculated using the Efthymiou parametric equations (Efthymiou, 1988), which remain the most widely used method for estimating SCFs in jacket fatigue analysis and are endorsed by design codes such as ISO 19902 (International Organization for Standardization, 2020) and API RP 2A-WSD (American Petroleum Institute, 2014).

Both the chord and the brace of a joint are considered separately, with each having eight hot-spot points. This results in a total of 16 SCF-adjusted stresses per joint, ensuring that the most critical fatigue location can be identified. The concentrated hot-spot stress at each location is determined from the nominal stress by applying the corresponding SCF, as expressed by:

$$f(\theta) = DAF(f_a[C_{ac}cos^2(\theta) + C_{as}sin^2(\theta)] + f_s C_{bs} sin(\theta) + f_c C_{bc} cos(\theta) \tag{11}$$

where, $f(\theta)$ is the concentrated stress at any point, *DAF* is the Dynamic Amplification Factor (if any), f_a, f_s and f_c are the nominal axial and bending stresses, C_{ac}, C_{as}, C_{bs} and C_{bc} are the SCFs for different stress components, and θ is the angle measured around the brace.

5.0 RESULTS AND DISCUSSION

The outputs from the spectral fatigue analysis are of paramount importance, as they provide several ways of identifying the critical joints and locations most susceptible to fatigue damage. In SACS, the results can be reviewed in two main formats:

i. Fatigue Listing File (ftglst):
A detailed numerical report that provides, for each joint, the calculated SCFs on both the brace side and chord side, the cumulative fatigue damage, the corresponding fatigue life, and the governing hot-spot location (e.g., crown, saddle, or chord face).

ii. Interactive Results Viewer (ftgext):
A graphical interface that allows engineers to visualise fatigue life distribution across the entire jacket, quickly identify critical joints and interactively explore "what-if" scenarios without rerunning the full spectral fatigue analysis.

5.1 Fatigue Listing File Results

Figure 13 shows an excerpt of the fatigue listing file for Joint 1117, presenting the full results for all braces framing into this joint. From this listing, the lowest fatigue life is 12.94 years, occurring at the chord face of Brace 1117-1015.

* * * MEMBER FATIGUE REPORT * * *
(DAMAGE ORDER)

JOINT	MEMBER ID	GRUP ID	TYPE ID	ORIGINAL OD (CM)	WT (CM)	JNT TYP	MEM TYP	CHORD LEN. (M)	GAP (CM)	* STRESS CONC. FACTORS * AX-CR	AX-SD	IN-PL	OU-PL	FATIGUE RESULTS DAMAGE	LOC	SVC LIFE
1117	1117-1015	DG2	TUB	40.64	1.270	TK	BRC	11.00	56.35	2.21	1.82	3.02	1.50	.3896525	B	51.32778
1117	1117-1121	LA1	TUB	90.00	5.489	TK	CHD	11.00		2.68	1.81	1.59	1.50	1.545707	B	12.93907
1117	1117-1063	HZ2	TUB	32.38	0.952	K	BRC	11.00	32.50	4.62	3.73	2.63	2.31	.6969661	B	28.69580
1117	1112-1117	LA1	TUB	90.00	5.489	K	CHD	11.00		4.28	3.04	1.99	1.84	.5230659	B	38.23610
1117	1117-1023	HZ2	TUB	32.38	0.952	TK	BRC	11.00	56.35	5.01	3.77	2.63	2.36	1.420528	T	14.07927
1117	1112-1117	LA1	TUB	90.00	5.489	TK	CHD	11.00		4.65	3.18	1.99	1.88	1.248236	T	16.02261
1117	1117-1093	XB1	TUB	32.38	1.270	K	BRC	11.00	32.50	2.57	1.91	2.97	1.50	.1492457	T	134.0872
1117	1112-1117	LA1	TUB	90.00	5.489	K	CHD	11.00		2.94	1.76	1.52	1.50	.2377122	T	84.13536
1117	1117-1075	XB2	TUB	32.38	1.905	TK	BRC	11.00	56.35	2.79	2.13	3.32	1.50	.1585262	T	126.1621
1117	1112-1117	LA1	TUB	90.00	5.489	TK	CHD	11.00		3.87	2.44	2.14	1.50	.5442610	T	36.74708

Figure 13 Excerpt from Fatigue Listing File – Results for Joint 1117

The fatigue life reported in the listing file is calculated from the damage using the relationship:

$$Fatigue\ Life = \frac{Design\ Life}{D} \tag{12}$$

For example, using a design life of 20 years and the damage value D = 0.3896525.

$$Fatigue\ Life = \frac{20}{0.3896525} \approx 51.33\ years$$

It can also be observed from the listing that the brace side and chord side produce different damage values and fatigue lives. This difference arises from:

- Different SCFs are calculated for each side, since separate parametric equations define brace-side and chord-side SCFs, and
- The thickness correction applied to the WJ S–N curve, which reduces the allowable stress range for members thicker than the 16 mm reference thickness. According to API RP 2A-WSD (American Petroleum Institute, 2014):

$$S = S_0 \left(\frac{t_{ref}}{t}\right)^{0.25} \tag{13}$$

where, S_0 is the allowable stress range from the base S–N curve, t_{ref} = 16 mm is the reference thickness and t is the actual member thickness. This correction shortens the predicted fatigue life for thicker chords, making the chord-side hot-spot governing in this case.

The numerical results are represented graphically in Figure 14, which highlights Joint 1117 in the global jacket model and visually identifies the connected braces and their calculated fatigue lives. This combined tabular and visual approach allows engineers to focus on the most critical locations immediately.

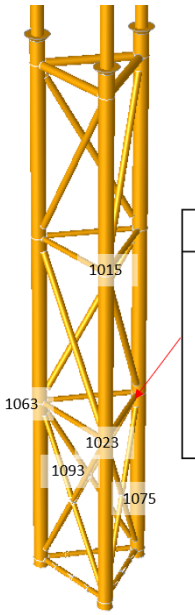

Joint	Life (years)	Brace Joint	B/C	Loc
1117	51.33	1015	BRC	B
	12.94		CHD	B
	28.70	1063	BRC	B
	38.24		CHD	B
	14.08	1023	BRC	T
	16.02		CHD	T
	134.01	1093	BRC	T
	81.14		CHD	T
	126.16	1075	BRC	T
	36.75		CHD	T

Figure 14 Fatigue life for Joint 1117.

Figure 14 presents the locations of the analyzed joints, specifically focusing on joint 1117. As shown, the governing location is the chord side of member 1117–1121 at the connection with brace 1117-1015, which yields the lowest fatigue life of 12.94 years. Although member 1117–1023 also shows a relatively low fatigue life on the brace side (14.07 years), it does not control the overall response. This is primarily because the cumulative damage at the 1117–1121 chord face is higher, a result attributed to the larger nominal loads transferred by diagonal brace 1117-1015 and the more severe thickness correction applied to the 5.489 cm chord wall. Consequently, the chord-side intersection at brace 1117-1015 remains the critical fatigue location for the structure.

5.2 Interactive Fatigue Viewer and Life Optimisation

The SACS interactive fatigue viewer (ftgext), shown in Figure 15, provides a powerful way to interrogate the fatigue results. Engineers can visualize fatigue lives across the jacket, review SCFs and governing hot-spot locations and even investigate potential design changes interactively.

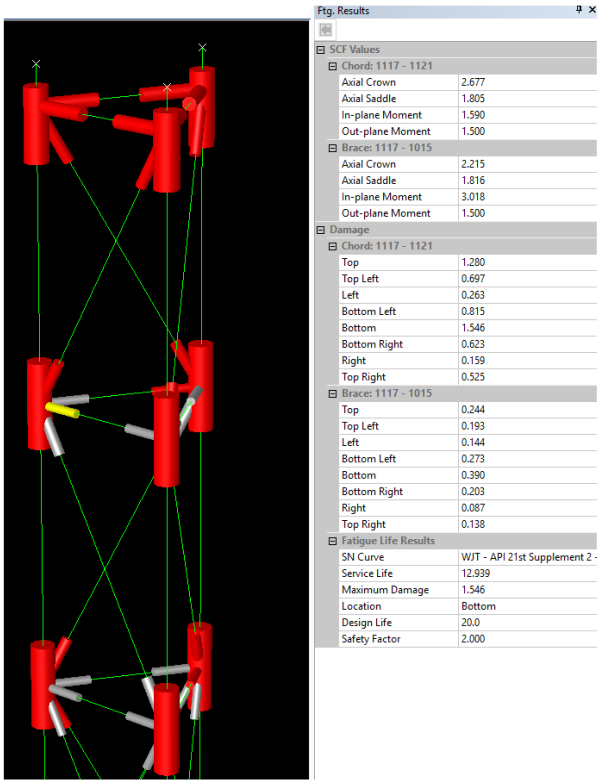

Figure 15 Chord 1117-1121 and Brace 1117-1015 result in FTGEXT.

For Joint 1117, the base case using the as-welded WJT curve predicts a fatigue life of only 12.94 years, which does not meet the typical 20-year design target. By upgrading the S–N curve to reflect weld improvement techniques, fatigue life can be significantly extended. Figure 16 illustrates this effect:

- WJ1 (weld profiling) increases fatigue life to 19.98 years, nearly achieving the target.
- WJ2 (weld-toe burr grinding) increases fatigue life further to 32.20 years, providing a substantial margin above the requirement.

The WJ2 curve represents a fabrication process where the weld toe is ground smooth to reduce the local stress concentration, delaying crack initiation and improving fatigue resistance.

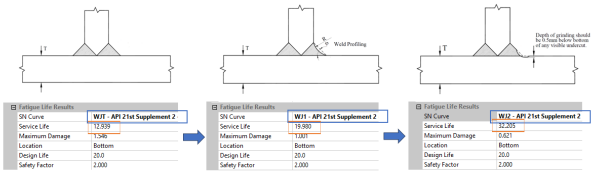

Figure 16 Weld improvement to increase fatigue life (Weld improvement figures modified from DNV RP C203 (DNV, 2017)).

This paper utilized the Efthymiou SCF formulation implemented in SACS (EFT), and the reported tubular joint fatigue results therefore correspond to weld-toe hot-spot stresses. Weld improvement factors (e.g., WJ1/WJ2) are consequently applicable when the governing fatigue damage is associated with weld-toe cracking. For tubular T, K, and Y type (TKY) brace to chord joints with single-sided weld details, weld-root cracking may govern and should be assessed separately using an approach appropriate for weld-root behavior. In SACS, this can be addressed using the EFR option, which applies Efthymiou-based SCFs with additional factors intended for single-sided weld root assessment, rather than relying solely on the EFT weld-toe hot-spot results.

6.0 CONCLUSIONS

This study presented a structured spectral fatigue analysis procedure for jacket-type offshore platforms, integrating theoretical principles with software implementation in SACS. Using a jacket in 54.5 m water depth as a case study, the workflow demonstrated how hydrodynamic model calibration, Centre of Damage (CoD) wave determination, soil–pile interaction linearization, transfer function generation, and dynamic response analysis provide the necessary inputs for fatigue life prediction.

The fatigue assessment identified Joint 1117 as the most critical location, with a predicted life of 12.93 years governed by the chord-side hot-spot. This outcome reflects the combined influence of brace–chord SCF differences and the thickness correction applied to the WJT S–N curve, which reduces allowable stress range for thicker members.

The methodology applies the Palmgren–Miner rule, together with Efthymiou-based SCFs, thickness-corrected WJT curves, and long-term metocean scatter data, ensuring full consistency with ISO 19902 and API RP 2A-WSD requirements. This approach provides a reliable basis for predicting fatigue life and reassessing existing assets.

From a design standpoint, the study demonstrates that weld improvement techniques (e.g., WJ1 weld profiling and WJ2 weld-toe burr grinding) can be implemented during fabrication to extend fatigue life and achieve design targets with a significant margin. From a structural integrity standpoint, the procedure enables targeted inspection planning and life-extension strategies by systematically highlighting fatigue-critical joints. These insights can guide retrofit, strengthening, or decommissioning decisions and help inform the design of future jacket structures to achieve improved fatigue resilience.

Acknowledgement

This research was funded by the Ministry of Higher Education under the Fundamental Research Grant Scheme [Grant Number: FRGS/1/2023/TK06/UTM/02/7] and by the Universiti Teknologi Malaysia (UTM) under UTM Fundamental Research [Grant Numbers: Q.K130000.3857.23H75], [Grant Numbers: Q.K130000.3814.22H97] which is gratefully acknowledged.

Conflicts of Interest

The author(s) declare(s) that there is no conflict of interest regarding the publication of this paper

References

[1] Abu Husain, M. K., Mohd Zaki, N. I., Mallahzadeh, H., & Najafian, G. 2014. Short-term probability distribution of the extreme values of offshore structural response by an efficient time simulation technique. *Ships and Offshore Structures,* 11(3): 286–299. DOI: https://doi.org/10.1080/17445302.2014.986877

[2] Ahmad Saharuddin, S. A., Dzulkifli, N. F. M., Mukhlas, N. A., Abu Husain, M. K., Mohd Zaki, N. I., Ahmad Shah, M. S., Umar, S., Teng, N. C., & Syed Ahmad, S. Z. A. 2024. Wave spectrum analysis for operational offshore platform in Malaysia water. *Malaysian Journal of Civil Engineering*, 36(2), 1–10. DOI: https://doi.org/10.11113/mjce.v36.22615

[3] American Petroleum Institute. 2014. *Recommended practice 2A-WSD: Planning, designing, and constructing fixed offshore platforms—Working stress design* (22nd ed.). American Petroleum Institute.

[4] Ayob, M. S., Kajuputra, A. E., Mukherjee, K. B., & Wong, S. 2014. Global ultimate strength assessment for existing offshore jacket structures (OTC-24938-MS). In Proceedings of the Offshore Technology Conference Asia, Kuala Lumpur, Malaysia, March 25–28. *Offshore Technology Conference*. DOI: https://doi.org/10.4043/24938-MS

[5] Azman, N. U., Abu Husain, M. K., Mohd Zaki, N. I., Mat Soom, E., Mukhlas, N. A., & Syed Ahmad, S. Z. A. 2021. Structural integrity of fixed offshore platforms by incorporating wave-in-deck. *Journal of Marine Science and Engineering,* 9(9): 1027. DOI: https://doi.org/10.3390/jmse9091027

[6] Damilola, O. J., Augustine, E. A., & Godspower, N. O. 2021. Fatigue evaluation of offshore steel structures considering stress concentration factor. *International Journal of Research and Review,* 8(10): 307–313. DOI: https://doi.org/10.52403/ijrr.20211041

[7] Defranco, S., O'Connor, P., Puskar, F., Bucknell, J. R., & Digre, K. A. 2010. API RP 2SIM: Recommended practice for structural integrity management of fixed offshore platforms. In *Proceedings of the Offshore Technology Conference*, Houston, TX, United States. Offshore Technology Conference. DOI: https://doi.org/10.4043/20675-MS

[8] DNV. 2017. *Recommended Practice: Fatigue Design of Offshore Steel Structures (RP-C203*). DNV [Retrieved September 17, 2025].

[9] Efthymiou, M. 1988 Development of SCF formulae and generalized influence functions for use in fatigue analysis. *Proceedings OT'88 "Recent Developments in Tubular Joints Technology". Surrey, UK.*

[10] Erfani, M. H. 2022. Structural Integrity Assessment of Offshore Jackets Considering Proper Modeling of Buckling in Tubular Members—a Case Study of Resalat Jacket. *Journal of Marine Science and Application,* 21(4): 145–167. DOI: https://doi.org/10.1007/s11804-022-00307-5

[11] Feng, Q., & Large, R. 2010. Prediction of Fatigue Life of Shallow Water Offshore Platforms Using Spectral Fatigue Analysis Method. *In Proceedings of the ASME 2010 29th International Conference on Ocean, Offshore and Arctic Engineering. Shanghai, China* 585–594. DOI: https://doi.org/10.1115/omae2010-20796

[12] International Organization for Standardization. 2020. Petroleum and natural gas industries — Fixed steel offshore structures (ISO 19902:2020). ISO. https://www.iso.org/standard/65688.html Retrieved January 12, 2026

[13] Jung, B.-H., Ahn, I.-G., Seo, S.-K., & Kim, B.-I. 2020. Fatigue Assessment of Very Large Container Ships Considering Springing Effect Based on Stochastic Approach. *Journal of Ocean Engineering and Technology,* 34(2): 120–127. DOI: https://doi.org/10.26748/ksoe.2020.012

[14] Kelma, S., & Schaumann, P. 2015. Probabilistic Fatigue Analysis of Jacket Support Structures for Offshore Wind Turbines Exemplified on Tubular Joints. *Energy Procedia,* 80: 151–158. DOI: https://doi.org/10.1016/j.egypro.2015.11.417

[15] Kraedegh, A. M., Lazar Jeremić, Igor Martić, Golubović, T., & Aleksandar Jovanović. 2024. Integrity and risk assessment of offshore jacket structures. *Structural Integrity and Life.* 24(3): 380–385. DOI: https://doi.org/10.69644/ivk-2024-03-0380

[16] Kvittem, M. I. 2014. *Modelling and response analysis for fatigue design of a semi-submersible wind turbine.* https://ntnuopen.ntnu.no/ntnu-xmlui/handle/11250/239262 Retrieved January 12, 2026

[17] Martínez, R. D. Á. B., Álvarez-Arellano, J. A., & Hamzaoui, Y. E. 2025. Assessment of structural integrity through On-Site Decision-Making analysis for a Jacket-Type offshore platform. *Applied Sciences*, 15(7): 3418. DOI: https://doi.org/10.3390/app15073418

[18] Mat Soom, E., Abu Husain, M. K., Mohd Zaki, N. I., M Nor, M. N. K., & Najafian, G. 2018. Lifetime Extension of Ageing Offshore Structures by Global Ultimate Strength Assessment (GUSA). *Malaysian Journal of Civil Engineering,* 30(1): 152-171 https://doi.org/10.11113/mjce.v30.174

[19] Mat Soom, E., Mohamad, M., Abu Husain, M. K., & Mohd Zaki, N. I. 2024. Probability of Failure for Fixed Offshore Structures Determination: An Analysis of a Braced Monopod and 4-Legged Platforms with Respect to Industry Standards. *Deleted Journal,* 3(1): 39–54. DOI: https://doi.org/10.24191/jscet.v3i1.39-54

[20] Moan, T. 2018. Life cycle structural integrity management of offshore structures. *Structure and Infrastructure Engineering*, 14(7): 911–927. DOI: https://doi.org/10.1080/15732479.2018.1438478

[21] Mohd Zaki, N. I., Abu Husain, M. K., & Najafian, G. 2014. Extreme structural response values from various methods of simulating wave kinematics. *Ships and Offshore Structures,* 11(4): 369–384. DOI: https://doi.org/10.1080/17445302.2014.987947

[22] Muis Alie, M. Z. 2016. The Effect of Symmetrical and Asymmetrical Configuration Shapes on Buckling and Fatigue Strength Analysis of Fixed Offshore Platforms. *International Journal of Technology,* 7(6): 1107. DOI: https://doi.org/10.14716/ijtech.v7i6.877

[23] Mukhlas, N. A., Mohd Zaki, N. I., Abu Husain, M. K., Syed Ahmad, S. Z. A., Ng, C. T., Ahmad Shah, M. S., Umar, S., & Md Noor, N. 2023. Prediction of Long-Term Offshore Structural Responses Based on Nonlinear Wave Modeling. *Journal of Sustainable Civil Engineering and Technology.* 2(2): 14–27. DOI: https://doi.org/10.24191/jscet.v2i2.14-27

[24] Nallayarasu, S., Goswami, S., Manral, J., & Kotresh, R. 2010. Spectral Fatigue analysis of jacket structures in Mumbai High Field. The *International Journal of Ocean and Climate Systems,* 1(3–4): 209–221. DOI: https://doi.org/10.1260/1759-3131.1.3-4.209

[25] Nicola, F. D., Graziano Lonardi, Fantuzzi, N., & Luciano, R. 2024. Structural integrity assessment of an offshore platform using RB-FEA. *International Journal of Structural Integrity*. 0: 1-39. DOI: https://doi.org/10.1108/ijsi-10-2023-0099

[26] Sarpkaya, T., & Isaacson, M. 1981. Mechanics of Wave Forces on Offshore Structures. *Van Nostrand Reinhold*, New York. ISBN 978-0-442-26412-8. DOI: https://doi.org/10.1016/0261-7277(82)90028-6

[27] Shabakhty, N., & Tabatabaei, S. S. 2021. Sensitivity of fatigue assessment for offshore jacket platform to different pile–soil–structure interaction models. *Ships and Offshore Structures*, 17(10): 2158–2175. DOI: https://doi.org/10.1080/17445302.2021.1979919

[28] Syed Ahmad, S. Z. A., Abu Husain, M. K., Mohd Zaki, N. I., Mukhlas, N. A., & Najafian, G. 2022. Extreme response prediction for fixed offshore structures by efficient time simulation regression procedures. Part 2: Model validation. *Ships and Offshore Structures*, 18(3): 414–422. https://doi.org/10.1080/17445302.2022.2059252

[29] Vuong, N. V., & Quan, M. H. 2019. Fatigue analysis of jacket support structure for offshore wind turbines. *Journal of Science and Technology in Civil Engineering (STCE) - NUCE,* 13(1): 46–59. DOI: https://doi.org/10.31814/stce.nuce2019-13(1)-05

[30] Wan Alwi, S. M. Y., Abu Husain, M. K., & Mohd Zaki, N. I. 2019. Marine growth inspection for jacket structures by behaviour and sensitivity analysis. In CRC Press eBooks. 586–596. CRC Press. DOI: https://doi.org/10.1201/9780429298875-67

[31] Wirsching, P. H. 1984. Fatigue reliability for offshore structures. *Journal of Structural Engineering,* 110(10): 2340–2356. DOI: https://doi.org/10.1061/(asce)0733-9445(1984)110:10(2340

[32] Yak, X. C., Mat Soom, E., Quen, L. K., Abu Husain, M. K., Azahar, M. A., Mohd Zaki, N. I., & Kang, H. S. 2022. Data science application in structural integrity analysis of fixed offshore jacket platform. *Journal of Physics Conference Series,* 2259(1): 012028. DOI: https://doi.org/10.1088/1742-6596/2259/1/012028

[33] Zhang, Z., & Sun, C. 2020. Structural damage identification via physics-guided machine learning: a methodology integrating pattern recognition with finite element model updating. *Structural Health Monitoring, 20(4):1675-1688* 147592172092748. DOI: https://doi.org/10.1177/1475921720927488

[34] Zwerneman, F., & Digre, D. 2010. 22nd Edition of API RP 2A Recommended Practice for planning, designing and constructing fixed Offshore Platforms – Working Stress Design. *Proceedings of Offshore Technology Conference*. DOI: https://doi.org/10.2523/20837-ms